The feedback of cold wakes on tropical cyclones

Kristopher B. Karnauskas[1, 2], Lei Zhang[1], Kerry A. Emanuel[3]

[1] Department of Atmospheric and Oceanic Sciences, University of Colorado Boulder

[2] Cooperative Institute for Research in Environmental Sciences, University of Colorado Boulder

[3] Department of Earth, Atmospheric and Planetary Sciences, Massachusetts Institute of Technology

Revised manuscript submitted to *Geophys. Res. Lett.*

March 12, 2021

Corresponding Author

Kristopher B. Karnauskas

University of Colorado Boulder

311 UCB / 4001 Discovery Drive

Boulder, CO 80309–0311

kristopher.karnauskas@colorado.edu

Abstract

Tropical cyclones (TCs) cause negative sea surface temperature anomalies by vertical mixing and other processes. Such cold wakes can cover substantial areas and persist for a month or longer. It has long been hypothesized that cold wakes left behind by intense TCs reduce the likelihood of subsequent TC development. Here we combine satellite observations, a global atmospheric model, and a high-resolution TC downscaling model to test this hypothesis and examine the feedback of cold wakes on subsequent TC tracks and intensities. Overall, cold wakes reduce the frequency of weak to moderate events but increase the incidence of very intense events. There is large spatial heterogeneity in the TC response, such as a southward shift of track density in response to cold wakes similar to that generated by Florence (2018). Cold wakes may be important for modeling and forecasting TCs, interpreting historical records and understanding feedbacks in a changing climate.

Key Points

- The effect of hurricane cold wakes on subsequent storms is tested using a combination of models and high-resolution satellite observations
- Cold wakes reduce the frequency of weak to moderate Atlantic storms, but increase the incidence of extremely intense hurricanes
- Cold wakes in the main development region have the greatest local impact, while those situated on its periphery induce latitudinal shifts

Plain Language Summary

Despite the increasing coastal vulnerability to hurricanes, several scientific barriers remain to realizing their full predictability. Chief among them is understanding the complex interactions between the atmosphere and ocean within a hurricane season. For example, hurricanes tend to form and strengthen

48 over warm water, but ocean mixing by their strong winds leave colder surface temperatures in their
49 wake. We modeled how cold wakes impact the next wave of hurricanes. We found that cold wakes
50 have a strong impact on subsequent hurricanes over a broad swath of the Atlantic Ocean. The cold
51 wake left by Hurricane Florence in September 2018, for example, reduced the likelihood of another
52 landfall along the entire U.S. east coast but increased its likelihood around the Caribbean.

1. Introduction

Tropical cyclones (TCs) derive energy from the heat content of the upper ocean. The mechanisms involved in this heat transfer include turbulent vertical mixing, upwelling, and evaporation (Liu et al., 2011; Price, 1981). As a direct result, TCs tend to leave behind a wake of cold sea surface temperature (SST) anomalies in their path (Leipper, 1967; Stramma et al., 1986), the effects of which on SST and stratification may last up to two months for major hurricanes (Hart et al., 2007). A recent example of such cold wakes, produced by 2018 Hurricanes Florence (Category 4) and Helene (Category 2), illustrates the spatial extent and temporal persistence of the SST anomalies generated by TCs (Fig. 1). In mid-September 2018, a cold wake with amplitude greater than 1°C could be detected continuously from the west coast of Africa near Dakar, Senegal to the east coast of the United States where Florence made landfall in North Carolina.

SST anomalies lying in the projected path of a TC, whether produced by previous TCs or otherwise, are of interest to hurricane forecasters because of their potential to modulate the intensity of the storm. Indeed, it has been shown that one TC can stunt the development of the next one by reducing the heat available to be drawn from the ocean (Balaguru et al., 2014). Furthermore, regional atmospheric circulations respond to tropical (Trenberth et al., 1998) and extratropical SST anomalies (Kushnir et al., 2002) in ways that may also influence hurricane development and motion through changes in vertical wind shear and steering flow. Besides case studies and statistical analyses of observations, a systematic modeling approach has not been applied to the hypothesis that TCs "self-regulate their activity … on intraseasonal time scales" (Balaguru et al., 2014). The goal of this study is to quantify the effect of cold wakes on the TC climatology of the North Atlantic basin including landfall probabilities.

Our approach, described in greater detail in the following section, combines high-resolution satellite SST observations, a global atmospheric general circulation model (AGCM), and a high-

resolution TC downscaling model to reveal the underlying ways in which a realistic set of cold wakes modify a baseline TC climatology of the North Atlantic. In this framework (Fig. S1), we are able to include not only the local impact of SST and upper-ocean stratification on TCs passing overhead, but the indirect effects of those SSTs on the broader, regional atmospheric circulation representing the environment through which the TCs are propagating. In the real world, there are typically 10 to 20 named TCs in the Atlantic basin per year. A significant advantage of this framework over conventional case-study modeling or statistical analysis of observations is the large number of synthetic TCs (thousands) that can be simulated in a small amount of time, which enables the unambiguous attribution of the responses to cold wake forcing including genesis, track and intensity.

2. Methods

2.1. Defining Cold Wakes

A set of SST anomalies characteristic of TC cold wakes were obtained based on satellite observations. We use the cold wakes produced by Hurricanes Florence and Helene in 2018, but our idealized modifications to the observed cold wake of Florence render it a suitable model representative of cold wakes in the North Atlantic rather than a limited case study.

The satellite observations used were from the Advanced Microwave Scanning Radiometer (AMSR), with 0.25° spatial resolution and 3-day averages. To obtain SST anomalies associated with cold wakes, we defined a 150 km radius around the National Hurricane Center (NHC) best track positions, extracted the minimum 3-day mean SST anomalies that occurred during the month of September 2018, interpolated onto the grid of the AGCM, and smoothed gently with a simple 9-point area average to avoid unnecessary granularity in the details of this particular event. The result of this process for Hurricanes Florence and Helene, on the final grid that both the AGCM and the TC downscaling are exposed to, can be seen in Fig. S2B–D. Comparison to the original satellite

observations (Fig. 1 and Fig. S3) confirms that the cold wakes as prescribed in the models are reasonable reproductions of the observations, and the various operations such as smoothing and regridding do not serve to exaggerate their size or amplitude.

In addition to the cold wakes as obtained from satellite SST observations following Hurricanes Florence and Helene, alternative cold wakes were produced by shifting the Florence wake northward and southward by approximately 7° latitude (Fig. S2E–F), scaling its amplitude by 0.5 (Fig. S2G), and linearly tapering its amplitude to approximately zero from the midpoint of the wake in the central Atlantic to the coast of Africa (Fig. S2H). Modeling these alternative cases enables exploration of the sensitivity of the results to such characteristics of a cold wake as latitude, amplitude, and zonal structure.

2.2. Global Atmospheric Modeling

The total, potential impact of an SST cold wake on a TC is not strictly through the local SST boundary condition, but also through the larger-scale atmospheric adjustment to the cold wake. A cold SST anomaly in the subtropical North Atlantic may, for example, alter (likely weaken) the vertical stratification of the atmosphere directly above (Ma et al., 2020). This may, then, have an influence on the atmospheric circulation (including vertical shear and steering-level winds) throughout the basin. Therefore, rather than simply exposing the TC downscaling model to cold wakes via the SST boundary conditions, we obtain the adjusted global atmospheric state in response to the same cold wakes using an AGCM, and then expose the TC downscaling model to both simultaneously. Our AGCM experiments are conducted using the Max Planck Institute (MPI) ECHAM version 4.6 (Roeckner et al., 1996) at T106 horizontal resolution (roughly 1° latitude by longitude) with 19 vertical levels up to 100 hPa. We conducted 25-year simulations (discarding the first 5 years as spinup) wherein our cold wakes as specified above (Fig. S2) were superimposed as anomalies on top of a seasonally varying SST

climatology that is otherwise identical across all of the AGCM experiments. The resulting solutions of these AGCM experiments defines the atmospheric environment to which the TC downscaling model was exposed.

2.3. Tropical Cyclone Downscaling

The TC downscaling model introduced by (Emanuel et al., 2008) is used. In this model, synthetic TCs are produced with a random seeding in space and time over the North Atlantic basin. The TC tracks are then predicted by a beta-and-advection model driven by the large-scale winds from the climate models. Along each track, a very high resolution, deterministic model is used for intensity prediction. This is an axisymmetric atmospheric model phrased in angular-momentum coordinates and coupled to a one-dimensional ocean model that simulates the effect of vertical mixing on SST. Thermodynamic and dynamic inputs to this intensity model are also obtained from the observationally-derived SST fields and AGCM solutions described above, including daily mean vertical wind shear between 250 and 850hPa, and monthly mean potential intensity, 600-hPa temperature, and specific humidity. We confirmed that a higher top AGCM configuration (70 hPa vs. 100 hPa) had no effect on potential intensity calculations or the results in general.

For each experiment, 4,000 synthetic TCs were generated through the random seeding process over the course of 20 years (where all SST and atmospheric inputs are the same in each year). Most seed vortices dissipate almost immediately; these are discarded. The survivors represent the downscaled TC climatology. For example, in the control run, 1,066,307 tracks were seeded to obtain 4,000 surviving TCs meeting the critical threshold wind speed of 40 knots, yielding 200 TCs per year for inclusion in the analysis. The annual frequency is determined by the ratio of the surviving seeds to the total number of seeds, multiplied by a constant determined by calibration with observations. This constant does not vary from one simulation to another. Although the basin was seeded randomly with

149 synthetic vortices, the TC climatology in the control simulation exhibits a realistic spatial pattern of
150 track density for both TCs and major hurricanes (Figs. S4–S5), consistent with previous analyses
151 (Emanuel, 2010; Emanuel et al., 2006, 2008). The TC downscaling model is run with different
152 combinations of SST forcing (with and without the presence of cold wakes) and large-scale
153 atmospheric parameters (as perturbed and not perturbed by cold wakes). We are thus able to estimate
154 the net impact of cold wakes on TCs, while disentangling the contribution of locally cooler SSTs from
155 that of remotely-driven atmospheric anomalies.

156 A final experiment with the TC downscaling model was conducted in which the subsurface
157 ocean was modified in terms of mixed layer depth and stratification. The standard "Florence"
158 experiment (not shifted, scaled, or tapered) was repeated, but with the mixed layer deepened by about
159 15 m and the stratification weakened by about 1.3°C per 100 m. These prescribed changes in mixed
160 layer depth and stratification were not spatially uniform; they were scaled by the local changes in SST
161 as observed (and prescribed), where the above values happen to accompany a 2°C SST cooling. These
162 prescribed changes were based on an average of *in situ* temperature profiles taken throughout the
163 passage of Hurricane Florence in September 2018 (Sanabia & Jayne, 2020).

164

165 *2.4. Diagnostics and mapping conventions*

166 Several TC-related metrics are calculated from the outputs of the TC downscaling model and analyzed.
167 Track density is defined as the number of TC tracks to propagate through a 1° latitude by longitude
168 grid cell per year, and are usually expressed as an anomaly relative to the control experiment. Genesis
169 density is as in track density but for the number of TCs to have their origin there (i.e., the first time a
170 seeded vortex reaches the critical wind speed of 40 knots).

171 The power dissipation index (PDI) is defined following (Emanuel, 2005) as

172 $$PDI = \int_0^{\tau} V_{max}^3 \, dt$$

173 where V^3_{max} is the maximum sustained wind speed at 10 m altitude and the integral is over τ, the
174 lifetime of the TC. Potential intensity V_{pot} is defined following (Bister, 2002) as

175 $$V_{pot}^2 = \frac{SST}{T_0} \frac{C_k}{C_D} [CAPE^* - CAPE]|_m$$

176 where T_0 is the outflow temperature, C_k is the exchange coefficient for enthalpy, C_D is the drag
177 coefficient, CAPE* is the convective available potential energy of air lifted from saturation at sea level
178 in reference to the environmental sounding, CAPE is that of boundary layer air, and subscript m
179 indicates evaluation at the radius of maximum winds.
180
181 **3. Results**
182 From a basinwide perspective, the prescribed cold wakes reduce the frequency of most TCs (Fig 2).
183 For example, the frequency decreases from about 11 TCs per year in the control simulation to 10 TCs
184 per year due to a single cold wake very similar to that produced by Hurricane Florence (2018). (We
185 actually simulate a fixed number of storms [200 in this case] per year. See Methods for how we
186 determine an annual frequency from the downscaling procedure.) This ~10% reduction is not critically
187 sensitive to most minor adjustments to the cold wake including tapering its amplitude to zero in the
188 eastern Atlantic, reducing its amplitude by a uniform 50%, or superimposing an additional wake
189 feature to the north mimicking that of Hurricane Helene (2018). In comparison, the latitude of the
190 cold wake has a far greater effect on its impact on TC frequency. When the cold wake is shifted to the
191 south by about 7° latitude, the reduction in frequency is much more pronounced—by 33% for all TCs
192 and by 40% or more for hurricanes. When the cold wake is shifted northward by the same distance,
193 its impact on TC frequency is diminished almost entirely. Examining the most intense (and rarest)
194 TCs reveals that the presence of a cold wake serves to *shorten* the return period of hurricanes whose

lifetime maximum wind speeds exceed 150 knots (a strong Category 5). The return period for hurricanes with maximum winds of 180 knots, for example, exhibit an approximately sixfold shortening—from 350 years to about 55 years—in the presence of a Florence-like cold wake.

There is spatial heterogeneity in the TC response (Fig. 3A). A Florence-like wake induces a broad reduction of TC track density (by about 1 TC per 1° grid cell per decade), which begins about 10° latitude south of the center of the cold wake and extends poleward throughout the domain where TC tracks are common. However, track density increases equatorward of 10° south of the cold wake. Overall, there is a southward shift of the climatological pattern of track density including a ~20% increase in the heart of the climatological maximum track density extending into the Caribbean (see Fig. S4E). These latitudinally-dependent results are echoed by changes in power dissipation (Fig. 3B) and landfall frequency (Fig. 3D). As there is no prescribed change in SST to the south of the cold wake, the increase in track density is explained by the change in genesis density (Fig. 3C) relative to the background potential intensity. There is a large horizontal gradient in the climatological potential intensity (Fig. S4B). The cold wake delays the development of westward propagating disturbances, thereby changing the location of genesis to one with a locally higher potential intensity, and feeding into a large-scale steering flow with more favorable conditions downstream. The possibility that potential intensity was increased to the south of the cold wake due to reduced heat flux to the atmosphere over the cold wake was investigated, but this was not the case and potential intensity indeed did not change by more than a few knots in the region south of the cold wake where track density increases.

Using the Florence-like cold wake as a general model but adjusting some of its characteristics further reveals the nature of the response of TCs to cold wakes in the North Atlantic. As hinted by the basinwide results, the latitude of the cold wake is a first order determinant of its probable impact on TCs. When the cold wake is shifted southward by 7°, the track density reduction is several times

219 stronger, and an adjacent track density increase is absent despite an increase in genesis density along
220 the extreme western Caribbean (Fig. 3E–G). The southward-shifted cold wake has a profound impact
221 on major hurricanes; the density of major hurricanes is locally reduced by over 50% (Fig. S6).
222 Conversely, an equivalent cold wake but shifted northward has a negligible impact on track density
223 anywhere in the domain (Fig. 3J). Given the baseline distributions of genesis density, track density and
224 potential intensity (Fig. S4–S5), it appears that a cold wake simply has a higher probability of making
225 an impact when it is in a region of high baseline TC activity. Relative to the original Florence-like cold
226 wake, changes in the amplitude, length, and shape of the cold wake have less control on the TC
227 response than does latitude (Fig. S7). Halving the amplitude of the cold wake lessens its impact without
228 changing the spatial pattern of the response. Shortening the length of the cold wake from either the
229 east or west causes modest changes to the zonal structure of the response without affecting its
230 meridional dependence, including the decrease in track density near the cold wake and the increase in
231 track density ~10° south of the cold wake.

232 The thousands of synthetic TCs propagating through this model framework are subject to
233 changes in both SST, which is a strong determinant of potential intensity, and to changes in the large-
234 scale atmospheric environment driven *by* SST changes (which alters vertical wind shear, stability, mid-
235 level humidity, potential intensity, and steering flow). Our sensitivity experiments wherein the TCs
236 "see" an SST field modified by a cold wake but simply the baseline atmosphere, and vice versa,
237 unequivocally show that the local SST anomalies are the primary cause of the results described thus
238 far (Fig. S8). The response of the atmospheric circulation over the North Atlantic to a cold wake—
239 even one as substantial as that produced by Florence in 2018—is simply not enough to override (or
240 contribute appreciably to) the changes in TC climatology induced by SST through potential intensity.
241 Our sensitivity experiment wherein the subsurface ocean was also modified with consistency to a cold
242 wake (deeper mixed layer and weaker stratification) does not differ qualitatively from the simulation

with a non-perturbed subsurface, but the amplitude of the response is smaller (Fig. S9). The impact of changing the subsurface scales with TC intensity; the largest alteration of the results due to subsurface modification is for major hurricanes. The reduction of basinwide major hurricane frequency due to the cold wake is roughly halved by the effect of the modified subsurface ocean.

Finally, we illustrate the potential societal importance of cold wakes by casting our results in terms of landfall events. Landfall frequency as a function of cold wake is highlighted for four representative coastal regions: the Carolinas, South Florida, the U.S. Gulf Coast, and the Lesser Antilles. There is a systematic tendency for cold wakes to reduce landfall frequency in these regions, spanning the intensity scale from tropical storms to major hurricanes (Fig. 4). For example, the control simulation exhibits 21 landfalling tropical storms per century in the Carolinas region; the presence of a cold wake like the one produced by Hurricane Florence reduces the probability of a subsequent landfall by 20%, or by over 50% for a similar cold wake but shifted southward by ~7°. The most profound change is in the Lesser Antilles, where the southward-shifted cold wake reduces the number of major hurricane landfalls from 14 per century to about 2.5 per century.

4. Summary and Discussion

The feedback of cold wakes on subsequent tropical cyclones was investigated using a modeling framework that accounts for the direct effect of SST anomalies on the potential intensity of TCs as well as the adjustment of the broader atmosphere to those SST anomalies. Overall, the existence of cold wakes reduces the frequency of weak to moderate events, but increases the incidence of very intense TCs (strong Category 5 storms). A possible explanation is an overshooting recovery of TCs that have been weakened by their passage over cold wakes; when TCs are weakened by an external influence, they churn up less cold water ahead of their current position, making them more intense once they do travel over that water. These results indicate that cold wakes are indeed important to

account for in operational forecasting and numerical modeling including investigations of the influence of climate forcing on TC risk.

These results appear to be roughly linear with magnitude of the wakes, but nonlinearly dependent on their latitude—relative to the region of high potential intensity and climatological track density. There is large spatial heterogeneity in the above TC responses, including the possibility of a north-south shift of probable tracks in response to a cold wake like the one Florence left behind in 2018. Such spatial shifts are possible because cold wakes can delay development, thereby changing the most likely region of genesis to one with a locally higher potential intensity and entrance point into the large-scale steering flow with more favorable conditions downstream. Most of the TC response to cold wakes is due to the direct effect of SST anomalies on TC intensity, with a very minor role for the broader atmospheric adjustment to the cold wakes. While SST anomalies lasting all season might change the circulation in ways that differ from those that last one month or less, we conclude that the large-scale atmospheric perturbations defined by the equilibrium AGCM response to cold wakes have a negligible impact relative to the direct SST forcing in the TC downscaling model.

Finally, several important questions of climate dynamics are inspired by these results. If not for the cold imprint of recent TCs left upon the ocean surface, would the closing months of the Atlantic hurricane season be on average more active? Is there a similar negative feedback involved in the response of TCs to anthropogenic global warming, such that warmer SSTs would lead to more frequent (and more intense) TCs, which produce more (and stronger) cold wakes, which would then inhibit further TC development? How strongly would such an effect counteract the *deeper* mixed layers typically found following the complete SST recovery and restratification? Along similar lines, do the presence of cold wakes obfuscate the observed correlations between temporal SST and TCs, since the canonical, expected direction of causality is from SST to TCs? Finally, do cold wakes in other regions such as the North Pacific have important effects on TCs? Other numerical modeling approaches are

possible, including ones with more robust representations of coupling to the ocean including the transient recovery of the mixed layer and persistent, anomalous ocean currents excited by the passage of storms.

Acknowledgements

Authors KBK and KAE received funding from the U.S. National Science Foundation (NSF), Prediction of and Resilience against Extreme Events (PREEVENTS), Awards 1854980 and 1854929.

Data Availability Statement

All data used as inputs to the models are publicly available online. The Advanced Microwave Scanning Radiometer (AMSR) satellite observations are available at http://www.remss.com/missions/amsr/. The *in situ* temperature profiles taken throughout the passage of Hurricane Florence in September 2018 by Sanabia & Jayne (2020) are available at http://argo.whoi.edu/alamo.html (all data) and https://accession.nodc.noaa.gov/0210577 (quality-controlled data).

304 **References**

305 Balaguru, K., Taraphdar, S., Leung, L. R., Foltz, G. R., & Knaff, J. A. (2014). Cyclone-cyclone
306 interactions through the ocean pathway. *Geophysical Research Letters*, *41*(19), 6855–6862.
307 https://doi.org/10.1002/2014GL061489

308 Bister, M. (2002). Low frequency variability of tropical cyclone potential intensity 1. Interannual to
309 interdecadal variability. *Journal of Geophysical Research*, *107*(D24), 4801.
310 https://doi.org/10.1029/2001JD000776

311 Emanuel, K. (2005). Increasing destructiveness of tropical cyclones over the past 30 years. *Nature*,
312 *436*(7051), 686–688. https://doi.org/10.1038/nature03906

313 Emanuel, K. (2010). Tropical cyclone activity downscaled from NOAA-CIRES Reanalysis, 1908–
314 1958. *Journal of Advances in Modeling Earth Systems*, *2*, 1.
315 https://doi.org/10.3894/JAMES.2010.2.1

316 Emanuel, K., Ravela, S., Vivant, E., & Risi, C. (2006). A Statistical Deterministic Approach to
317 Hurricane Risk Assessment. *Bulletin of the American Meteorological Society*, *87*(3), 299–314.
318 https://doi.org/10.1175/BAMS-87-3-299

319 Emanuel, K., Sundararajan, R., & Williams, J. (2008). Hurricanes and Global Warming: Results from
320 Downscaling IPCC AR4 Simulations. *Bulletin of the American Meteorological Society*, *89*(3), 347–
321 368. https://doi.org/10.1175/BAMS-89-3-347

322 Hart, R. E., Maue, R. N., & Watson, M. C. (2007). Estimating Local Memory of Tropical Cyclones
323 through MPI Anomaly Evolution. *Monthly Weather Review*, *135*(12), 3990–4005.
324 https://doi.org/10.1175/2007MWR2038.1

325 Kushnir, Y., Robinson, W. A., Bladé, I., Hall, N. M. J., Peng, S., & Sutton, R. (2002). Atmospheric
326 GCM Response to Extratropical SST Anomalies: Synthesis and Evaluation*. *Journal of*

Climate, *15*(16), 2233–2256. https://doi.org/10.1175/1520-0442(2002)015<2233:AGRTES>2.0.CO;2

Leipper, D. F. (1967). Observed Ocean Conditions and Hurricane Hilda, 1964. *Journal of the Atmospheric Sciences*, *24*(2), 182–186. https://doi.org/10.1175/1520-0469(1967)024<0182:OOCAHH>2.0.CO;2

Liu, J., Curry, J. A., Clayson, C. A., & Bourassa, M. A. (2011). High-Resolution Satellite Surface Latent Heat Fluxes in North Atlantic Hurricanes. *Monthly Weather Review*, *139*(9), 2735–2747. https://doi.org/10.1175/2011MWR3548.1

Ma, Z., Fei, J., Lin, Y., & Huang, X. (2020). Modulation of Clouds and Rainfall by Tropical Cyclone's Cold Wakes. *Geophysical Research Letters*, *47*(17). https://doi.org/10.1029/2020GL088873

Price, J. F. (1981). Upper Ocean Response to a Hurricane. *Journal of Physical Oceanography*, *11*(2), 153–175. https://doi.org/10.1175/1520-0485(1981)011<0153:UORTAH>2.0.CO;2

Roeckner, E., Arpe, K., Bengtsson, L., Christoph, M., Claussen, M., Duemenil, L., et al. (1996). The atmospheric general circulation model ECHAM-4: Model description and simulation of present-day climate.

Sanabia, E. R., & Jayne, S. R. (2020). Ocean Observations Under Two Major Hurricanes: Evolution of the Response Across the Storm Wakes. *AGU Advances*, *1*(3). https://doi.org/10.1029/2019AV000161

Stramma, L., Cornillon, P., & Price, J. F. (1986). Satellite observations of sea surface cooling by hurricanes. *Journal of Geophysical Research*, *91*(C4), 5031. https://doi.org/10.1029/JC091iC04p05031

Trenberth, K. E., Branstator, G. W., Karoly, D., Kumar, A., Lau, N.-C., & Ropelewski, C. (1998). Progress during TOGA in understanding and modeling global teleconnections associated

with tropical sea surface temperatures. *Journal of Geophysical Research: Oceans*, *103*(C7), 14291–14324. https://doi.org/10.1029/97JC01444

354 **Figures**

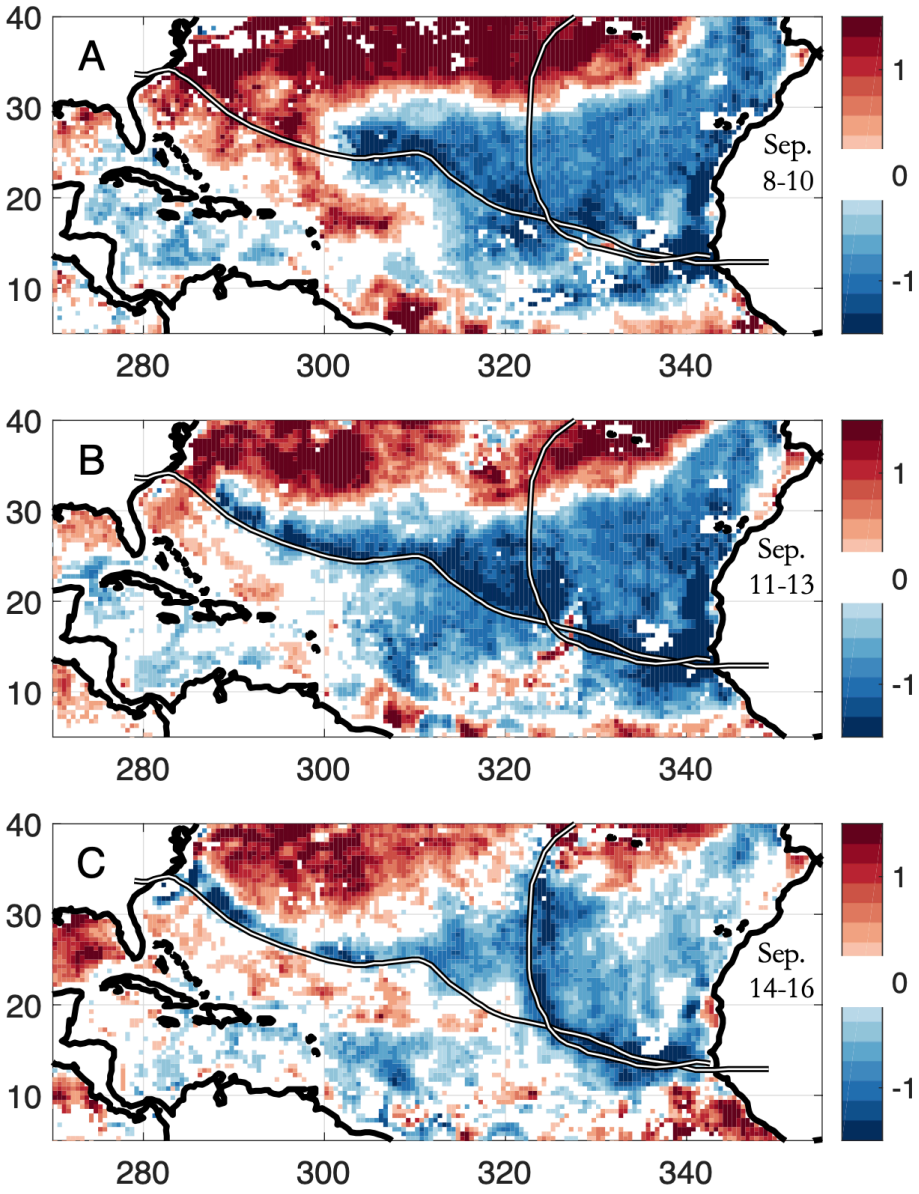

355

356 **Figure 1.** Sea surface temperature anomaly averaged from (A) 8–10, (B) 11–13 and (C) 14–16
357 September 2018. Anomalies are relative to the same three calendar days averaged over 2002–2017.
358 Data from the Advanced Microwave Scanning Radiometer (AMSR)–E (2002–2011) and AMSR–2
359 (2012–2018). For this figure, AMSR data were linearly interpolated onto a 0.5° grid (from the original
360 0.25° product). Values less than ± 0.25°C are masked (white). See Methods for more details.

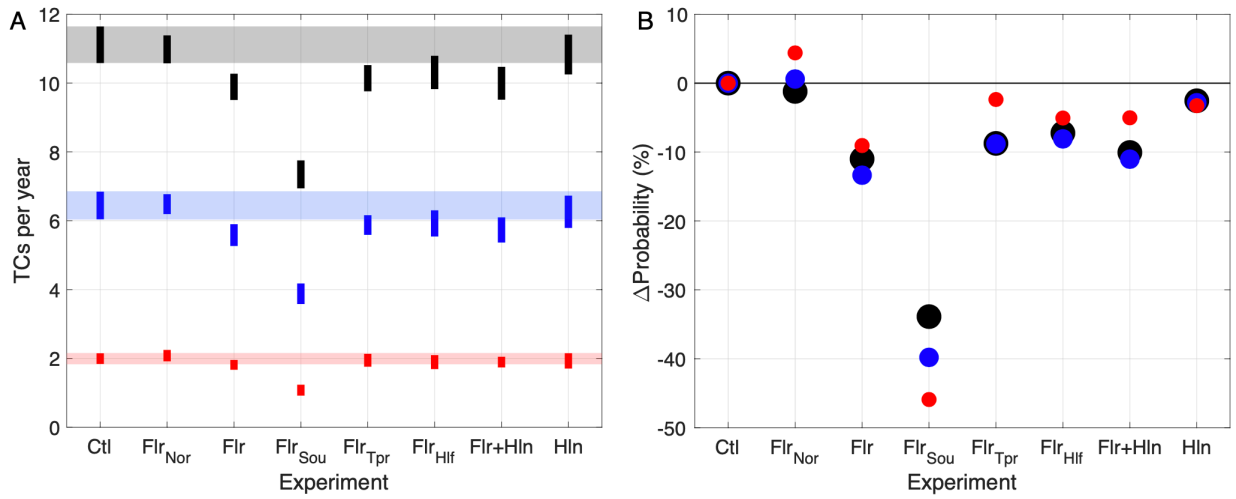

Figure 2. (A) Mean annual number of TCs (black), hurricanes (blue) and major hurricanes (red) in the control simulation (labeled Ctl on the x-axis) and all wake experiments. Bar heights represent the 90% confidence intervals on the mean values (transparent shaded bars simply extend the 90% confidence intervals on the control mean values across the entire plot for comparison). (B) As in (A) but normalized such that each mean value is expressed as a percent difference from the control mean value for each intensity classification. Wake experiments labeled Flr_{Nor}, Flr_{Sou}, Flr_{Tpr}, and Flr_{Hlf} represent northward shifted, southward shifted, tapered (to zero in the east), and uniformly halved (in amplitude) variants on the Florence (Flr) wake, respectively. Wake experiments labeled Flr+Hln and Hln represent both Florence and Helene wakes simultaneously present, and only the Helene wake present, respectively. See Fig. S2 for a depiction of the SST forcing associated with each of these experiments.

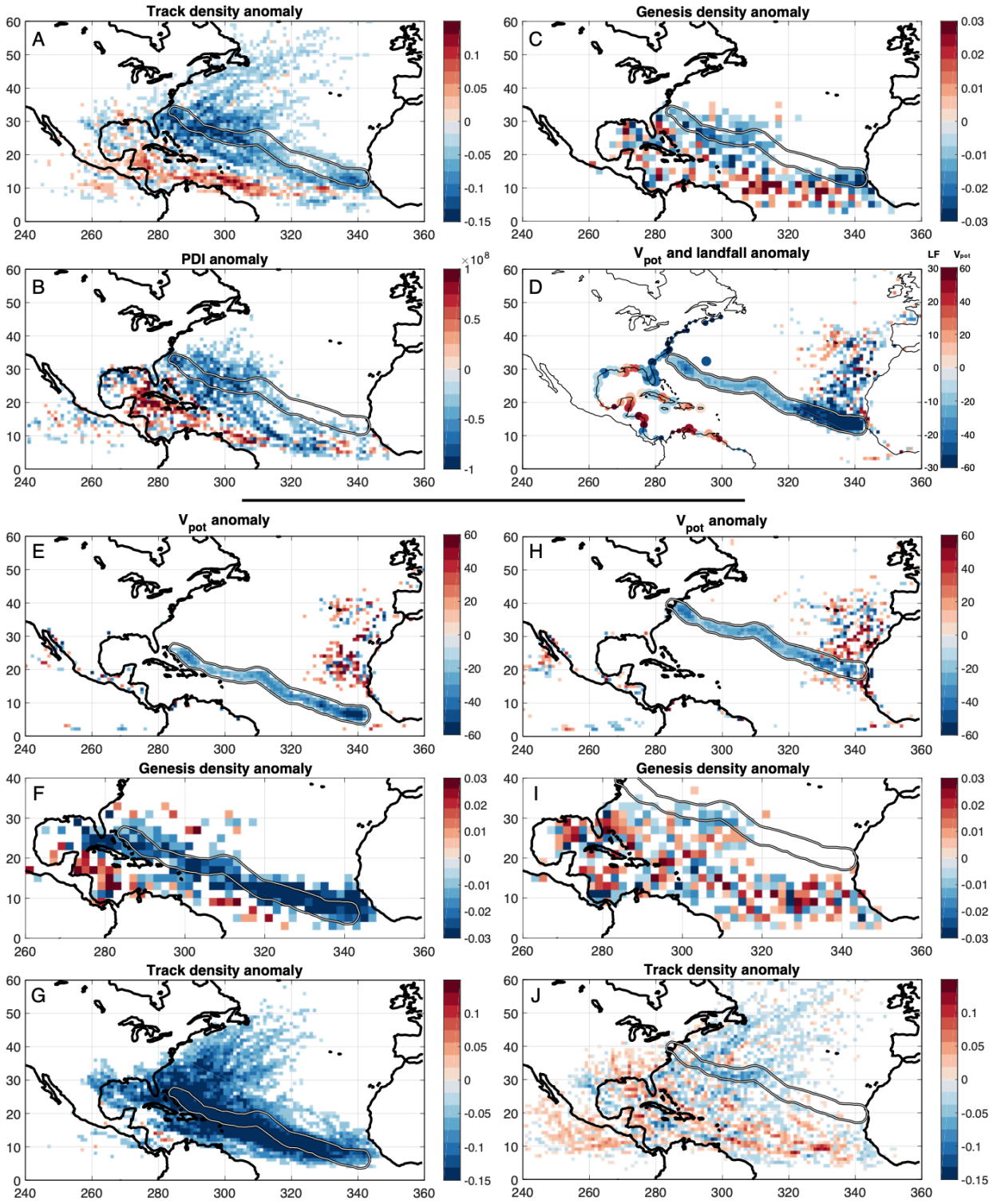

372

373 **Figure 3.** Anomaly maps for (A) track density (TCs per 1° grid cell per year), (B) power dissipation

374 index (PDI; m^3s^{-2}), (C) genesis density (TCs per 2° grid cell per year), and (D) potential intensity (V_{pot};

375 knots) and landfall frequency anomaly (bubbles along the North and South American coastline; %

376 change). Landfall bubble size is proportional to the annual number of landfalls per year in the control
377 simulation. (E–G) Potential intensity anomaly (knots), genesis density anomaly (TCs per 2° grid cell
378 per year) and track density anomaly (TCs per 1° grid cell per year) for the Florence-South wake. (H–
379 J) as in (E–G) but for the Florence-North wake. All anomalies are relative to the control simulation.
380 The –0.5°C SST anomaly isotherm of the applicable wake is contoured on each panel for reference.

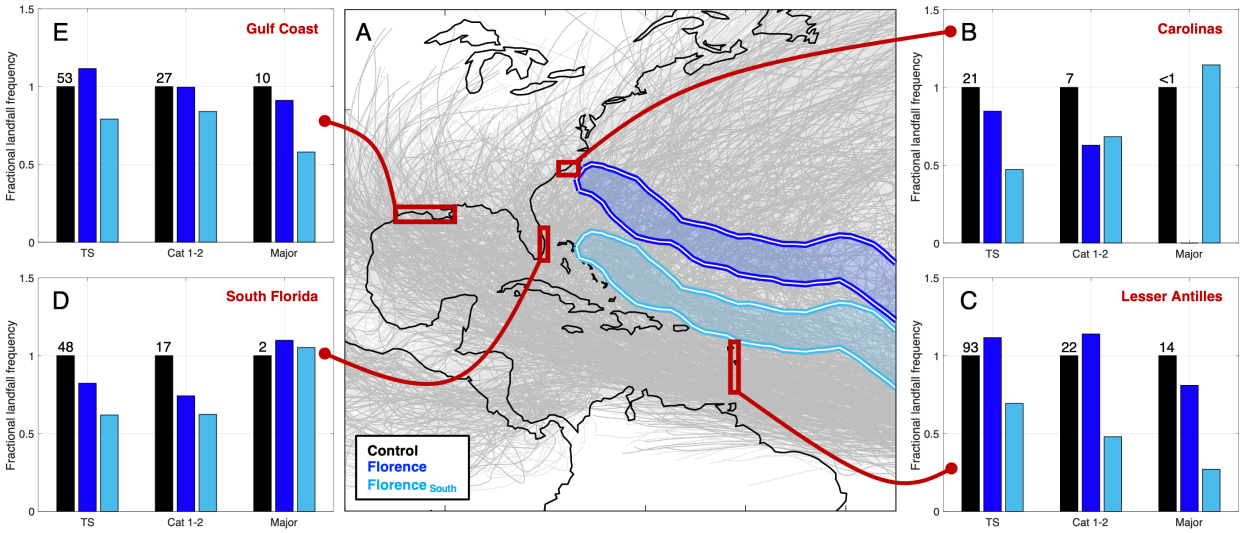

Figure 4. (A) Overview map of the Atlantic basin with all 4,000 synthetic TC tracks generated in the control simulation (darker gray for major hurricanes), the –0.5°C SST anomaly isotherms associated with the Florence (royal blue) and Florence-South (light blue) wakes, and four representative coastal regions highlighted. (B) Fractional landfall frequency results at the Carolinas coastal region (extending roughly from Morehead City, NC to Myrtle Beach, SC) for three different intensity classifications (tropical storms, category 1–2 hurricanes, and major hurricanes [category 3+]) and three different experiments (control, Florence wake, and Florence-South wake). All bars are expressed as fractions of the control simulation results. Control results (numbers of landfalls per century) for each intensity classification are listed above each control bar. (C–E) as in (B) but for the Lesser Antilles region, South Florida region and the northwestern U.S. Gulf Coast region, respectively.